EXPLOITING COUPLED JOINTS
Anatomic Control of the Spine with IK Through Linearly Coupled Joints

Daniel Raunhardt and Ronan Boulic

VRLAB, Ecole Polytechnique Fédérale de Lausanne, 1015 Lausanne, Switzerland

Keywords: Inverse kinematics, joint coupling, human modeling, articulated figure.

Abstract: In this paper we propose a simple model for the coupling behavior of the human spine that is capable of exhibiting anatomically correct motions of the vertebrae in virtual mannequins. Such a model transparently integrates in our inverse kinematics framework as it couples standard swing and revolute joint models. The adjustment of the joints due to the coupling is made with several simple (in)equality constraints, resulting in a reduction of the solution space dimensionality for the inverse kinematics solver. A key benefit is to prevent the inverse kinematics algorithm from providing infeasible postures. We exploit how to apply these simple constraints to the human spine by a strict decoupling of the swing and twist motion of the vertebrae and demonstrate the validity of our approach on various experiments.

1 INTRODUCTION

Realistic animations of human characters play an important role for interactive applications. Three dimensional virtual mannequins are the common representation of the graphical interface, serving as an interactive character inside the virtual environment (Magnenat-Thalmann et al. 2004) (Philips et al. 1990). Often researchers improved the representation and animation of the exterior skin and muscle deformations of the virtual mannequins (Wilhelms et al. 2002) while the model of the underlying body has been kept unchanged. However, increasing the surface details of the virtual mannequins may lead the viewers to be more sensitive to unrealistic joint motions in animations such as in the shoulder and spine regions of the human body (Hodgins et al. 1998).

Joint models are important for correct motion analysis of tasks, including the estimation of muscle lengths and moment arms (Delp et al. 1995). Introducing accurate biomechanical joint models to the traditional hierarchy of joint transformations can lead to an improved realism in human character animation. Anatomical axes of rotations and joint centers of the human body are taken from literature and refined to produce improved fidelity of the motions.

   In this paper we introduce a human spine model based on a set of coupled vertebral joints that reflect its anatomic mobility distribution (Kapandji 1982a)(Kapandji 1982b). The vertebral joints are coupled through linear equality constraints allowing to transparently integrate the spine model within an existing inverse kinematics (IK) solver. Each equality constraint reduces the solution space for the inverse kinematics solver. Relatively few parameters are necessary to control the complex articulation of the human spine. We give a short introduction to our inverse kinematics solver based on the Prioritized Inverse Kinematics (Baerlocher et al. 2004) and demonstrate the validity of our model with different experiments including performance measurements.

2 PREVIOUS WORK

The first use of articulated joint models for representing human joints can be found in studies of kinematics of robotic manipulators. These systems used the Denavit-Hartenberg link parameter notation from robotics to represent virtual mannequins with articulated limbs (Girard et al. 1985). Although the notation to associate coordinate frames between adjacent segments is convenient, each parameter set describes only a single degree of freedom (dof) between two segments. Multiple dofs can be achieved by combining multiple sets of parameters. Structures like the spine exhibit a high degree of

coupling behavior. This coupling behavior of the spine has been exploited by Monheit et al. (1991) to develop a kinematic model of the spine that exhibits flexion-extension, lateral bending and axial torsion rotation. For a normalized representation of the human skeleton Kulpa et al. (2005) modeled the spine with a spline that could be divided into segments. To retrieve the positions of the vertebrae, the spline representing the spine is simply discretized according to the distances of the vertebrae.

Apart form the spine itself, Maciel et al. (2002) incorporate joints that can translate and rotate together on plane and where the joint limits dynamically change with the dofs of any joint. Herda et al. (2005) characterize the joint coupling behavior by implicit surfaces obtained from motion captured values. This representation allows to characterize intra- and inter-joint dependencies but is not a very intuitive way to control the human motion of the joints. To restrict the joint angle ranges for ball-and-socket joints spherical polygons (Korein 1985) and joint sinus cones (Maurel et al. 2000)(Wilhelms et al. 2002) have been introduced. Spherical polygons are more general than cones but they are also more complex to deal with. Cones are often sufficient to represent the human joints (Korein 1985).

Like our approach the Peabody system (Badler et al. 1993) collects joints into different groups of joints that have group angles to configure the joint groups' segments. Shao et al. (2003) introduced a general joint component model called joint maps that allows modeling of joint expressions over several bone segments for biomechanical accurate joints. A joint map is a function that takes a set of inputs (e.g. set of joints) to produce output for one or more joints. The input can be seen as the dofs and the outputs are the modified joint values (e.g. angle, translation variations). The outputs of one joint map can be combined with the inputs of another joint map to create increasingly sophisticated behaviors. The process that performs this mapping varies according to the type of the desired joint behavior.

Seen from this variety of presented joint models, a single joint model representation is not suitable for capturing all the different characteristics of the human joints. In fact, specialized joint models are often needed.

In contrast our model uses common joint models such as revolute (1 dof) or swing (2 dofs) joints for inverse kinematics. Through coupling we group the joints into sets and reduce the remaining solution space for the inverse kinematics solver. The paper focuses especially on the case of the spine but it can

be used for a wide range of other cases. The spine case is especially interesting because the mobility allowed by the vertebrae shape is changing all along the spine. For this reason we separate the handling of the swing and the twist components. This allows producing anatomically correct postures.

3 PRIORITIZED INVERSE KINEMATICS

3.1 Constraining the Solution

We provide here only a brief overview of the Prioritized Inverse Kinematics algorithm (PIK) that handles an arbitrary number of priority levels and linear constraints for the purpose of controlling virtual mannequins or robot manipulators. In this approach the articulated structure is organized as a tree of chains. In the specific case of the human body we are compliant with the H-Anim standard (Humanoid Animation Working Group) that includes all human joints.

As the joint models are independent of each other, possible coupling, due to the presence of tendons or muscles spanning over several joints, is defined as additional "hard" constraints. This is achieved through equality constraints acting on the coupled joint parameters. We exploit also inequality constraints for two purposes: to model the limit range of a single joint or to offer a "relaxed" coupling between joints.

Let us recall the definition of linear equality (Figure 1 left) and inequality constraints (Figure 1 right) for a joint configuration q with n dofs:

$$c_i^T q = b_i \text{ for } i = 1..g \qquad (1)$$

$$c_i^T q \leq b_i \text{ for } i = 1..g \qquad (2)$$

where the c_i are n-dimensional vectors and the b_i are scalars. Equation (2) allows simple lower bounds and upper bounds on joint variables, as well as linearly coupled joint limits. This set of constraints defines a convex space of feasible configurations. The choice of linearity is due to the higher complexity introduced by non-linear constraints. Joint limits that should never be violated are handled as inequality constraints while we model the anatomical joint coupling generally by equality constraints.

The general PIK algorithm relies on an efficient computation of projection operators enforcing tasks grouped into an arbitrary number of strict priority levels. The management of the (in)equality constraints must be integrated within the process that computes the joint variation. Ignoring the constraints for the computation of the joint variation and only

adjusting the resulting joint configuration to satisfy the constraints leads to non optimal solutions (Baerlocher et al. 2004). The linear equality constraints can be ensured within a single iteration step at the initialization phase of the joint variation computation. To achieve this we modify the initial projection operator P_0 so that the resulting solution space lies on the constrained subspace. Secondly, the initial joint variation, noted Δq^0, is set to the displacement required to meet the constraints, if this is not already the case. This second term helps also to avoid numerical drift away from the constraints. Compared to the PIK algorithm described in (Baerlocher et al. 2004), these additional "hard" constraints can be seen as tasks of "infinite" priority (i.e. of higher importance than any other task) shaping the solution space. The initial projector operator P_0 remains constant as long as no equality constraint is added or removed.

```
procedure init_projector
begin
      P₀ = Iₙ
      for all equality constraint do
            if (¬conflicting constraint)
                  P₀ = P₀ - P₀(c*cᵀ)
            end if
      end for
end
```
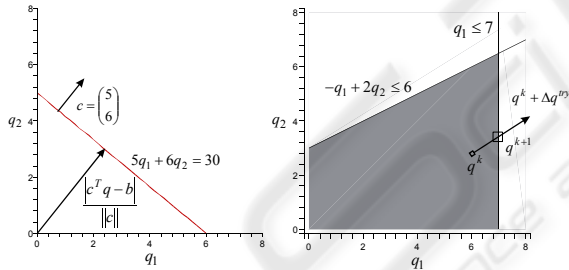

Figure 1: Left: equality constraint between two joints q_1 and q_2. Right: the grey region indicates the possible area of solutions for the joints q_1 and q_2. The computed solution $q^k+\Delta q^{try}$ violates the inequality constraint $q_1 \leq 7$, so the corrected solution is clamped to q^{k+1}.

The inequality constraints are checked after the new joint configuration q^{k+1} is computed, where the new joint state is defined as the sum of the current configuration and the computed solution $q^k+\Delta q$. Figure 1 (right) illustrates a case where the new configuration violates an inequality constraint modeling a joint limit; therefore a new equality constraint is dynamically added into the constraint set, called the working set, to clamp the corresponding joint on the limit. In our model we check first the user-defined inequality constraints

and afterwards the joint limits. This gives the user-defined inequality constraints a higher priority over the joint limits. The prioritized solution is re-evaluated as long as no additional inequality constraint is violated (Figure 2). This loop is necessary to guarantee the tasks' error minimization. The cost of the clamping loop is linear to the number of recruited joints (see section 3.2). In the worst case each clamping iteration would handle a single clamped joint. This is seldom the case as, very often multiple joints violate their limit simultaneously which is handled through a single clamping iteration.

If two (in)equality constraints are conflicting, i.e. they cannot be satisfied at the same time, we consider only the constraint that has been first added to the working set of the constraints (e.g. the user-defined inequality constraints dominate the joint limits). Thus, we may get a solution of the joint variation that may violate some of the constraints.
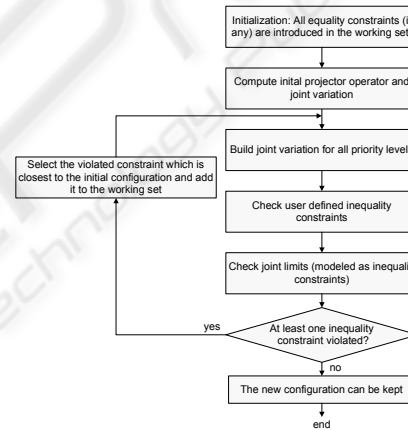

Figure 2: The Prioritized Inverse Kinematics convergence loop highlighting the construction of the joint variation solution for multiple priority levels and the management of the equality and inequality constraints.

3.2 Joint Recruiting Level

Our PIK allows a task to *recruit* all or part of the joints from its parent up to the root of the articulated structure. We can manually discard joints that should not participate to achieve the task. For example, whenever controlling the position of the wrist it is important to decide whether the spine should participate or not. The problem of overlapping joint regions has first been described by Badler et al. (1980). Normally to resolve this problem a minimal joint recruiting rule for joints shared by multiple tasks has to be enforced (Le Callennec et al. 2006). This rule concerns those parts of the articulated structure where multiple tasks may recruit part of their joints. Let T_i be a task of priority

i, $Rec(T_i)$ the corresponding set of recruited joints and $Anc(T_i)$ all the possible joints that may be recruited by T_i (from its parent up to the root). Then, for any two priority levels $a>b$ we must have:

$$Rec(T_b) \cap Anc(T_a) \subset Rec(T_a) \qquad (3)$$

Equation (3) states that recruited joints of low priority tasks are a subset of high priority tasks. Without this rule, it may lead to diverging solutions where a low priority task dominates a high priority task. Equation (3) solves the problem of overlapping regions only if there are no joints coupled by (in)equality constraints. The first problem using coupled joint is that joints can be implicitly recruited. If a joint is recruited by the task T_i and if this joint is also coupled to other joints, all these coupled joints are implicitly recruited by task T_i. A joint recruited by a low priority task can be coupled to a joint that is only recruited by high level priority task. Thus, the low priority task would gain influence over the high priority task despite Equation (3) is satisfied. The set of all implicitly recruited joints due to coupling of a task T_i is defined as $Coup(Rec(T_i))$. The second problem is that joints are coupled that are not recruited by any task. Thus, we extend the Equation (3) to the following conditions for the recruiting level for any two priority levels $a>b$:

$$(Rec(T_b) \cup Coup(Rec(T_b))) \cap (Anc(T_a) \qquad (4)$$
$$Coup(Rec(T_a))) \subset Rec(T_a)$$
$$\bigcup Coup(Rec(T_i)) \subset \bigcup Rec(T_i) \qquad (5)$$

Equation (4) ensures that coupling can only take place from the joints up to the root of the articulated structure and that a lower priority task cannot couple a joint that is nearer to the root than a higher priority task. Equation (5) states that only joints recruited by task are allowed to be also coupled by constraints.

4 SPINE

4.1 Introduction

The human spine consists of twenty four movable vertebrae. According to positions and the functionality of the individual vertebrae, the spine can be divided into three sets: the cervical region (seven vertebrae in the neck), the thoracic region (twelve vertebrae in the thorax), and the lumbar region (five vertebrae in the abdomen) (Kapandji 1982a) (Kapandji 1982b) (Monheit et al. 1991). Each vertebra has three dofs of rotation (flexion-extension, lateral-bending and torsion). These three rotational components may have quite different rotation centers and non-orthogonal rotation axes.

Modeling each vertebra as a joint without taking into consideration the coupling that exists among them due to the rotational behavior is not recommended as too much freedom is left in the spine for the inverse kinematics solver. This choice usually leads to unrealistic spine postures. It is preferable to use only a few uncoupled joints strategically placed on the spine, in order to have a more realistic rigidity of the system. Thus, we simplify the control of the spine movement by a simple reduction of the dofs.

4.2 Spine Model

As each vertebra allows a swing motion (flexion-extension, lateral-bending) and a torsion motion (rotation along vertical vertebrae axis) the general solution would be to represent each vertebra by a ball-and-socket joint (3 dofs). Euler angles, quaternions or exponential maps are often used to express these segment orientations. The use of quaternions or the exponential map for inverse kinematics is advantageous compared to Euler angles as they have no singular configuration within their mobility range (Grassia 1998). For this reason our inverse kinematics solver represents the joints as exponential maps. The drawback of the exponential map for the coupling with linear (in)equality constraints is that it would not be possible to couple independently the swing components or the twist of two ball-and-socket joints as by changing the swing of a ball-and-socket joint the torsion of this joint may be changing too. To control separately the swing and twist of the joints we have chosen to consider two distinct joint types: swing (2 dofs) and revolute (1 dof). The swing joint model is an exponential map vector with zero contribution along the main spine axis (no twist). It models the flexion/extension and lateral bending of the vertebrae while the revolute joint is oriented along the spine main axis to model the twist mobility (also called the torsion). These joints are strategically placed over the spine as seen in Figure 3. Owing to this organization we obtain a great flexibility in the coupling schemes. For example, we may couple the torsion of a joint with the lateral-bending of another as happens in the cervical spine (White et al. 1990). Thus, we are able to fully control the coupled behavior of the spine by two common joint models and simple (in)equality constraints.

For interoperability we have chosen to use the same joint names as defined in H-Anim (Humanoid Animation Working Group). As in the lumbar region the torsion is equally distributed (Kapandji 1982a)(Kapandji 1982b) and its amount is very small, we have placed only one revolute joint in this region. In the thoracic and the cervical region we

have placed more revolute joints according to the corresponding bigger torsion ranges. The concrete coupling coefficients are based on the vertebrae value ranges and their human coupling behavior (Kapandji 1982a)(Kapandji 1982b). Table 1 presents our choice of the joint ranges based on our strategically placed joints over the spine.

Table 1: Joint ranges of the spine at different levels of the spine along the three anatomic axis (Kapandji 1982a) (Kapandji 1982b).
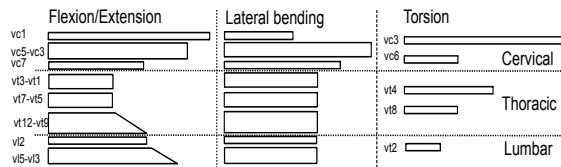
To keep some independent movement between the individual regions of the spine (lumbar-thoracic, thoracic-cervical) we couple two regions with inequality constraints as illustrated in Figure 3. This helps the regions to behave more independently than with a strict coupling by equality constraints. Nevertheless we can ensure a fluent transition between two regions.
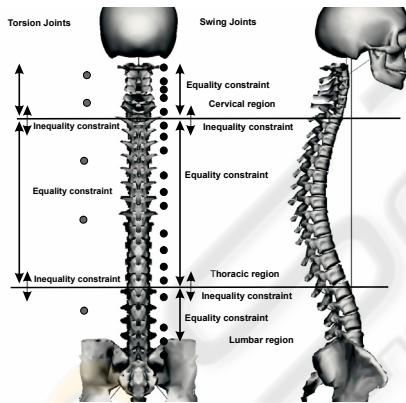

Figure 3: Our human spine model with the different spine regions. We have strategically placed some rotational joints (indicated by gray circles) to model the torsion of the spine where for the remaining joints we use swing joints (indicated by black circle). Inside a region we couple the swing joints by equality constraints. To keep some independency between the regions we use inequality constraints.

The problem that arises with this concept is that the equality constraints and the inequality constraints (user-defined for the regions or joint limits) may be conflicting. To avoid such conflicting we do only check the joint limits for the first joint in each spine region (for swing: vl5, vt12, vc7; for twist: vl2, vl8, vc6). The accordance to the joint limits of the other

joints is automatically given by the use of real measured vertebrae value ranges and human coupling coefficients. The drawback of inequality constraints is that they can lead to a re-evaluation of the joint variation solution.

4.3 Summary

To summarize, our spine model is composed of three segments. We strictly decouple the swing and twist of the vertebrae using only swing and revolute joints. Within each segment we couple the joints by equality constraints, while the different segments are connected by inequality constraints. A simple joint coupling with equality constraints inside each spine region would leave only 3 dofs (1 for flexion/extension, 1 for lateral bending and 1 for torsion) to each region. This would make a total of 9 dofs to control the entire spine which is considerably less than the 72 dofs in an uncoupled spine. Although our model is probably still not as accurate as a real human spine, we can achieve fairly more realistic spine configurations than in an uncoupled spine. We think that our spine model is a good compromise between the accuracy and the simplicity of control.

5 RESULTS

5.1 Isolated Spine

This experiment highlights the behavior of our approach with two conflicting tasks on an isolated spine consisting of 24 vertebrae where the vertebrae are coupled with 32 equality and 12 inequality constraints. Figure 4 on the left shows the initial configuration of the spine. We have defined a position and an orientation task to be achieved. The orientation task is modeled as a high priority task while the position task has low priority. We executed this experiment twice, once with the coupled spine and once where the joints of the spine can move independently within their independent joint limits.

Figure 4 highlights the initial position, the achieved configuration for the spine without coupling and with coupling. The obvious problem of the uncoupled spine is the strong change of the spine shape while the coupled spine displays no abrupt changes of the shape. This behavior of the uncoupled spine is possible due to the lack of coupling, each joint being able to move independently without taking into account the motion of other joints. We have also compared the computational speed, the error convergence and the

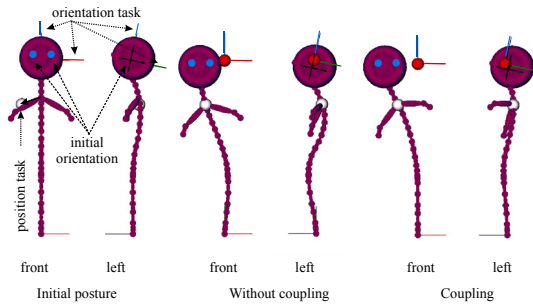norm of the joint variations of the two methods (Figure 5).

Figure 4: Front and left side views of the isolated spine: (left) initial configuration with indications of the two tasks; (middle) end configuration without coupling; (right) end configuration with coupling.
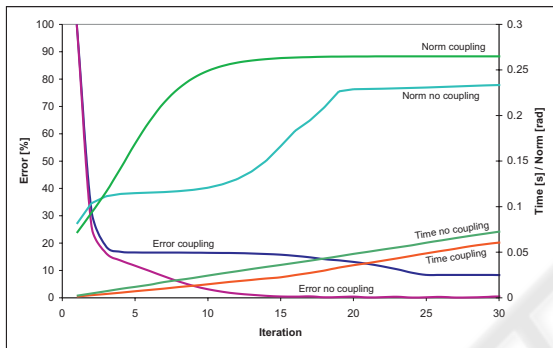

Figure 5: Comparison between coupling/no coupling for computational time and error convergence.

Coupling with equality constraints reduces the solution space for the inverse kinematics solver. Therefore the error convergence could be slowed down or the task may not be achievable while without coupling it would be possible. In this experiment the position task with coupling cannot be fully achieved, so the final error does not converge to zero. Overall the total computational time shows some advantages for our coupling approach. By the pre-computation of the initial projection operator the computational overhead is limited to adjusting the initial joint variation before each iteration. We have measured that around 3-8% of the total computational time for one iteration are spent to initialize the joint variation. But as we remove some dofs for the inverse kinematics solver this computation stage is cheaper; in the end we gain some computational time compared to the approach without coupling (cf. "Error no coupling" and "Error coupling" curves in Fig. 5). Due to coupling we also restrict the overall joint variation during the convergence (cf. "Norm no coupling" and "Norm coupling" curves in Figure 5).
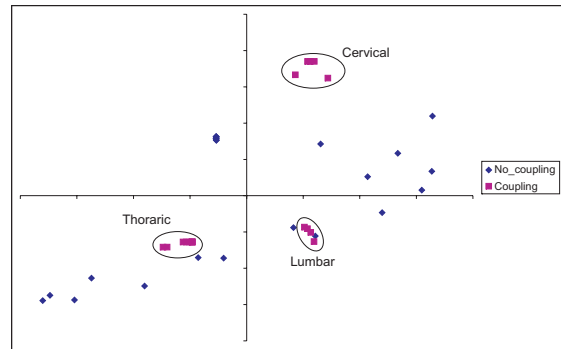

Figure 6: Distribution of the swing components of the vertebrae for coupling/no coupling.

The swing components s_x (flexion-extension) and s_y (lateral-bending) are presented in Figure 6. The swing component values without coupling are widely distributed in the s_x-s_y space which leads to the change of the signs in the spine as presented in Figure 4 in the middle. On the other hand the swing component values of the vertebrae with coupling are grouped per spine region and can only change significantly between two regions. Another problem of the uncoupled spine is the abrupt change of the torsion direction which is discussed in detail in Section 5.2.1.

5.2 Full Body Postures

A spine model of 24 vertebrae may be too time consuming for real-time applications of virtual mannequins especially if there are other time consuming calculations such as skinning or collision detection/response. Thus, a simplified spine model is often used. In the next experiments the uncoupled simplified spine consists of 8 ball-and-socket joints with a total of 24 dofs. The lumbar and the thoracic region are each represented with three joints while the cervical region has only two joints. As already mentioned our coupled spine model can only be represented by swing and rotation joints. Our coupled spine model is built by 8 swing joints and 5 rotational joints. Figure 7 illustrates the initial posture for the next experiments.

5.2.1 Bio-mechanical Considerations

In this experiment the virtual mannequin with the simplified spine has to achieve a simple balanced posture. The toes of the right foot are attracted toward a position in the back while the hands have to reach a position in the front. These goals are modeled with a middle priority position task. During the whole motion the left foot has to stay on the ground which is reflected by two high priority tasks (one for the toes and one for the heel). A low

priority orientation task is used to maintain the head looking forward. To keep the virtual mannequin in balance we project the center of mass over the left foot with the highest priority task. We executed this experiment twice, once with our coupling approach and once with independent vertebrae (Figure 7 right).
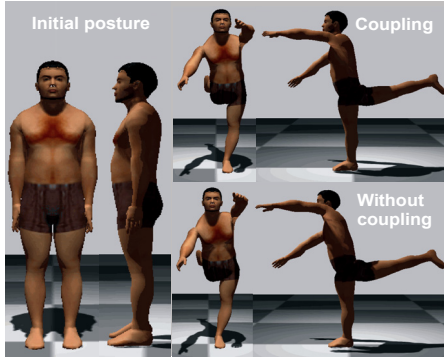

Figure 7: The initial and the achieved postures without coupling and with coupling.

Although both methods are visually similar there is an important difference. In the uncoupled spine there is an abrupt change in the torsion direction. Considering three successive vertebrae (Figure 8 left), the lowest vertebrae may have a torsion to the right, the middle to the left while the third vertebrae rotates again to the right.
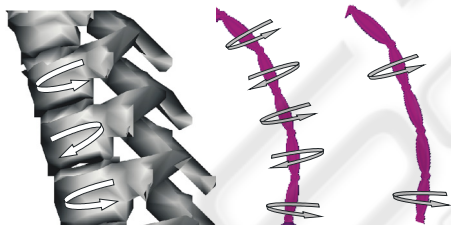

Figure 8: Possible changes of the torsion direction of vertebrae for an uncoupled spine (left) and corresponding measured values for uncoupled spine (middle) and coupled spine (right).

We have measured a similar behavior of the vertebrae torsion directions for the uncoupled spine as illustrated in Figure 8 middle. Such a behavior is bio-mechanically not possible although a change of the torsion direction is possible between spine regions.

For the coupled spine changes of the torsion direction can only appear for vertebrae which are coupled by inequality constraints (e.g. between two spine regions).

5.2.2 Periodic Tasks

This experiment highlights the behavior of coupling for long periodic tasks. The hands of the virtual mannequin have to follow a moving goal which forms an eight in the vertical plane (two low priority positional tasks are used). The feet have to stay on the ground (four high priority tasks) and the virtual mannequin has to keep its balance by projecting the center of mass between the two feet (highest priority task). Figure 9 illustrates the different postures without coupling and with coupling after an increasing number of cycles.
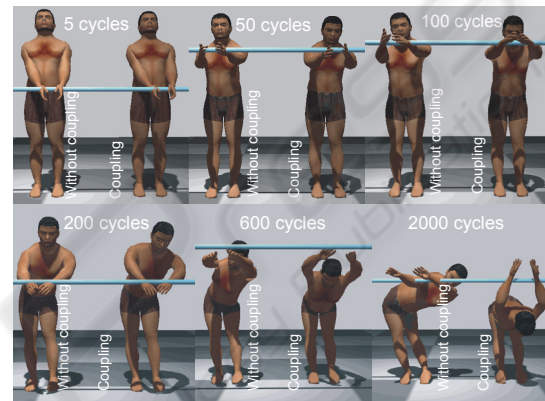

Figure 9: Postures on the left without coupling and on the right with coupling after an increasing number of cycles (from left to right and top to bottom). The blue bar indicates the goal of the hands.

At the beginning the two postures are almost identical. We can observe that the differences between the postures increase with the number of cycles. After 2000 cycles the coupled spine has still a plausible shape while the uncoupled is highly deformed. This is caused by the drift of the solution in the joint space as originally discussed by Klein et al. (1983). Coupling joints by (in)equality constraints reduces the solution space for the inverse kinematics solver which counteracts this drift in the joint solution space for periodic tasks.

6 CONCLUSIONS

In this paper we have proposed a simple method to model the coupling behavior of the spine. We use simple (in)equality constraints to reflect the coupling between the vertebrae. Each equality constraint removes one dof of the solution space for the inverse kinematics solver. Relatively few parameters are sufficient to represent the spine. We have shown that our approach is able to produce more natural spine

shapes. By introducing constraints the inverse kinematics solver may be no longer able to find a solution with the same error as without coupling due to the reduced solution space. The coupling may be too restrictive and not cover the whole space of possible human spine motion but it provides plausible postures of the spine and is less sensitive to the drift of the solution for periodic tasks. Besides the computational cost is slightly less than for the uncoupled one. Our future work is to exploit this model within a real-time posture control of a virtual mannequin interacting with its environment.

ACKNOWLEDGEMENTS

REFERENCES

Badler, N. I., O'Rourke, J., Kaufman, B. 1980. Special problems in human movement simulation. In *Proceedings of the 7th Annual Conference on Computer Graphics and Interactive Techniques* (Seattle, Washington, United States, July 14 - 18, 1980). SIGGRAPH '80. ACM Press, New York, NY, 189-197.

Badler, N. I., Phillips, C. B., Webber, B. L. 1993. *Virtual Humans and Simulated Agents*. New York, NY: Oxford University Press.

Baerlocher, P., Boulic, R. 2004. An Inverse Kinematics Architecture Enforcing an Arbirtray Number of Strict Priority Levels. In *The Visual Computer,* Springer Verlag, 20(6), 402-417.

Delp, S.L., Loan, P. 1995. A software system to develop and analyze models musculosketal structures, *Computers in Biology and Medicine*, vol. 25, 21-34.

Girard, M., Maciejewski, A. A. 1985. Computational modeling for the computer animation of legged figures. In *Computer Graphics (SIGGRAPH 1985 Proceedings)*, B. A. Barsky, Ed., vol. 19, 263-270.

Grassia, F. S. 1998. Practical parameterization of rotations using the exponential map. *J. Graph. Tools* 3, 3 (Mar. 1998), 29-48.

Herda, L., Urtasun, R., Fua, P. 2005. Hierarchical implicit surface joint limits for human body tracking. *Computer Vision and Image Understanding* 99(2), 189-209.

Hodgins, J. K., O'Brien, J. F., Tumblin, J. 1998. Perception of Human Motion With Different Geometric Models. *IEEE Transactions on Visualization and Computer Graphics* 4, 4 (Oct. 1998), 307-316.

Humanoid Animation Working Group, 1999, H-Anim 1.1 specification for a standard humanoid. www.h-anim.org.

Kapandji, I. A. 1982 a. *The Physiology of the Joints: Upper Limb*, 2 ed., vol. 1. Churchill Livingstone.

Kapandji, I. A. 1982 b. *The Physiology of the joints : The Trunk and the Vertebral Column*, 2 ed., vol. 3. Churchill Livingstone.

Klein, C. A., Huang, C. H. 1983. Review of pseudoinverse control for use with kinematically redundant manipulators, *IEEE Transactions on Systems, Man, and Cybernetics*, Vol. SMC-13, No-2 (March/April), 245-250.

Korein, J. U. 1985 *A Geometric Investigation of Reach*. MIT Press.

Kulpa. R., Multon F., Arnaldi B. 2005. Morphology-independent representation of motions for interactive human-like animation. *Computer Graphics Forum* 24, 3 (2005), 343-352.

Le Callennec, B., Boulic, R. 2006. Interactive motion deformation with prioritized constraints. *Graph. Models* 68, 2 (Mar. 2006), 175-193.

Maciel, A.; Nedel, L.P.; Dal Sasso Freitas, C.M. 2002. Anatomy-based joint models for virtual human skeletons, *Computer Animation, 2002. Proceedings of* , vol., 220-224.

Magnenat-Thalmann, N., Thalmann, D. 2004. *Handbook of Virtual Humans*. Wiley. ISBN 0-470-02361-3.

Maurel, W., Thalmann, D. 2000. Human shoulder modeling including scapulo-thoracic constraint and joint sinus cones. *Computers and Graphics 24*, 2, 203--218.

Monheit, G., Badler, N. I. 1991. A Kinematic Model of the Human Spine and Torso. *IEEE Comput. Graph. Appl.* 11, 2 (Mar. 1991), 29-38.

Phillips, C. B., Zhao, J., Badler, N. I. 1990. Interactive real-time articulated figure manipulation using multiple kinematic constraints. In *Proceedings of the 1990 Symposium on interactive 3D Graphics* (Snowbird, Utah, United States). SI3D '90. ACM Press, New York, NY, 245-250.

Shao, W., Ng-Thow-Hing, V. 2003. A general joint component framework for realistic articulation in human characters. In *Proceedings of the 2003 Symposium on interactive 3D Graphics* (Monterey, California, April 27 - 30, 2003). SI3D '03. ACM Press, New York, NY, 11-18.

White, A. A., Panjabi M.M. 1990. *Clinical Biomechanics of the Spine*, Philadelphia, J.B. Lippincott Company, ISBN 0-397-50720-8.

Wilhelms, J. Gelder, A. V. 2002. Fast and easy reach-cone joint limits. *J. Graph. Tools* 6, 2 (Sep. 2002), 27-41.